DEVELOPMENT OF A REUSABLE TIMBER-CONCRETE-COMPOSITE SYSTEM FOR BRIDGE DECKS

James P. Wacker[1], Joana A. A. Campos[2], Alfredo M. P. G. Dias [3]

ABSTRACT: This paper highlights research results from a joint effort between the Forest Products Laboratory (FPL) in the United States of America (USA) and the University of Coimbra (UC) in Portugal (PT). The main objective is the development of a Timber-Concrete Composite system (TCC) that utilizes precast concrete deck panels that accelerate construction times and can easily be removed to facilitate bridge repair/rehabilitation efforts and reuse options. The research is focused on various critical aspects such as the type of interconnection between the concrete deck and the glued laminated timber beams or the interconnection between the precast concrete deck panels. Several practical requirements were addressed that are important to the bridge industry in Portugal and in the USA, such as: accelerated bridge construction time, cost-competitiveness with existing bridge solutions, and eliminating the need for specialized labour skills.

KEYWORDS: Timber-concrete, bridges, composite structures, reuse, disassembling

1 INTRODUCTION

TCC systems have been widely used all over the world for almost one century. Early examples of the use of this technology on bridges are reported in the USA in the early 1920's [1]. The potential of this TCC solution is well known in various aspects, for example: promotes more efficient mechanical performance, achieves higher durability, and reduces the environmental impacts [2, 3].

The objective of this research is the development of solutions to new bridge decks, eventually suitable for rehabilitation works. Throughout the project two bridge solutions were studied, the first solution is a single lane bridge and the second solution is a bridge with two traffic lanes. The one-way solution was studied in the laboratory. A bridge deck was tested with a span of 10.00m, a total width of 7.00m comprising of a 3.50m (one-way) carriageway, 0.50m roadside, and 1.50m sidewalks. The preliminary analysis considered actual conditions that are to be found in both USA and Europe in practice. In terms of design, both European and the USA bridge design code requirements were considered [4-10].

The analysis included both experimental and numerical results that were obtained with FEM numerical models.

2 NUMERICAL WORK

Numerical analysis was carried out to complement experimental work. In these analyses, FEM models were used to simulate the mechanical performance of both the deck components and the global deck. An example of a model is shown in Figure 1. The analytical approaches were based on numerical work from previous researches [11].

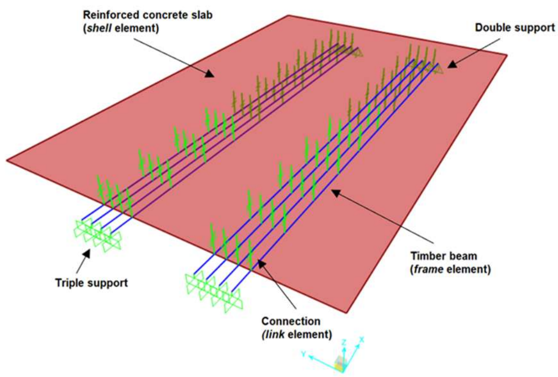

Figure 1: *FEM numerical model*

At an early stage, the numerical results were used to base the decision on the configuration of the TCC specimens. At a later stage, the models were validated using the experimental results obtained in this research.

[1] James P. Wacker, USDA Forest Products Lab, USA, james.p.wacker@usda.gov
[2] Joana A. A. Campos, ISISE, University of Coimbra, Portugal, uc2007107964@student.uc.pt
[3]Alfredo M. G. P. Dias, ISISE, University of Coimbra, Portugal,
alfgdias@dec.uc.pt

Adjustments were introduced in the models in order to obtain a better simulation of the TCC deck actual performance. The improved models were then used to simulate other conditions such as new load combinations or new configurations.

The bridge deck was modelled using *frame* elements to define the timber beams, *shell* elements to model the reinforced concrete slab, and *link* elements to model the connection between timber and concrete. In the analysis, both materials, timber and concrete were modelled assuming linear elastic behaviour.

3 EXPERIMENTAL WORK

In this type of structural system, the numerical models can be very effective and allow a good insight in their mechanical performance. However, they are not (yet) accurate enough to validate a practical application in such demanding conditions [2]. The aspects that do require experimental assessment refer to both components and the composite bridge deck superstructure. A rather critical component in such a solution is the connection systems [12]. The experimental work was divided into two phases, the first phase related to the study of the TCC connections, and the second phase with the study of the TCC bridge deck superstructure.

The connection configuration was developed based on bibliographic, analytical, and experimental analysis. The connection assessment included single shear push-out tests performed in real size specimens for various practical loading conditions, namely, static loads, cyclic loads, and fatigue loads.

In the second phase, a full-scale TCC bridge deck with a one-way span length of 10m was produced and tested in the lab. This specimen was also tested with static and cyclic loads in order to allow a better insight of its performance in service. After the tests, the TCC specimen will be decommissioned in order to show the potential of these systems in terms of repairing techniques and ease of re-purposing the bridge components.

Additionally, all the components and materials were tested in order to characterize them and obtain accurate properties that are required as input for numerical models. This assessment includes both physical and mechanical properties.

3.1 SHEAR TESTS ON TCC CONNECTIONS

The connection assessment included single shear push-out tests performed in real size specimens for a variety of loading conditions: static loads, cyclic loads, and fatigue loads.

The static loads were designed to determine the ultimate load carrying capacity and the slip modulus. The cyclic and fatigue loads were intended to evaluate the connection performance, namely its stiffness and strength when a high number of cyclic loads was applied. Globally, 6 static loads, 4 cyclic loads, and 2 fatigue load protocol tests were performed.

3.1.1 DESCRIPTION OF TESTS

The single shear push-out test specimens consist of a precast concrete element and two side-by-side pieces of timber (these joined transversely by threaded rods). The connection between timber and concrete, whose schematic drawings are given in Figure 2 and Figure 3, consists of an asymmetric notch, a connector (thread rod + washer + hex nut), and a steel plate in each timber element.

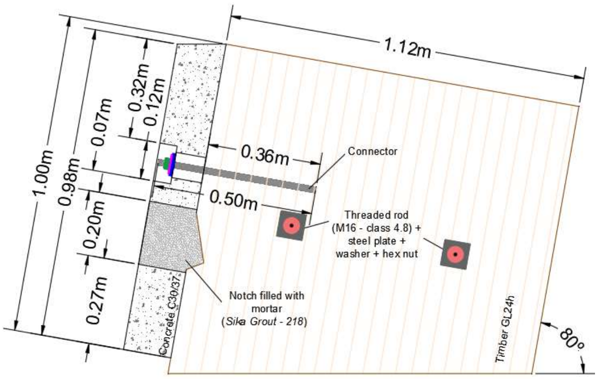

Figure 2: *Connection configuration - side view*

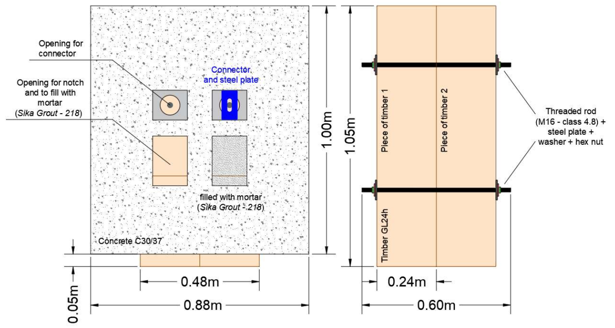

Figure 3: *Connection configuration – front view*

Timber used in the test pieces was GL24h strength class glued laminated timber with a cross-section of 0,24 m x 1,12m.

Concrete used in the precast concrete panels of the specimens was C30/37 ready-mixed concrete from which cubes with 0,15m of edge were obtained to perform compression tests. In the concrete element, with 0,15m of thickness, top and bottom reinforcement mesh was used. The mesh was constituted by 5Ø16 (five steel bars with a diameter of 16mm) in the transversal direction and 3Ø10 (three steel bars with a diameter of 10mm) in the longitudinal direction. The steel for reinforcement concrete used was A500NR.

The connection was made up of thread rod M20- strength class 8.8 + washer + hex nut, and a steel plate (70x130x12mm), and the notch was filled with a one-component, fluid, shrinkage-compensated mortar (*Sika Grout-218*).

The transversal joining of the two side-by-side pieces of timber was carried out using two M16 threaded rods of strength class 4.8 + steel plate (80x80x6mm) + washer + hex nut. The steel plate was used to prevent crushing on timber elements.

The execution of the specimens was carried out essentially in 3 stages. In the first stage the precast concrete elements were built, the formwork was made with the negatives for the connection, the reinforcement was placed and the pouring of concrete was carried out.

In the second stage, the timber pieces were prepared, more specifically with the cut of the timber pieces at the ends, the opening of the notches, and the transverse holes (with a diameter of 18mm), followed by the union between the timber pieces (see Figure 3).

Subsequently, holes were made for placing the connector (with a diameter of 24mm), after which, they were filled with epoxy resin (two-component structural epoxy ligant - *Sika Icosit K 101N*) and the threaded rod positioned and keep fixed for 24 hours until the glue could get stuck.

Finally, the assembly was made between the timber pieces and the precast concrete element, that is, the slab was placed on top of the two timber beams in the proper position and the opening in the slab and the notch in the beams was filled with *Sika Grout-218* (see Figure 4).

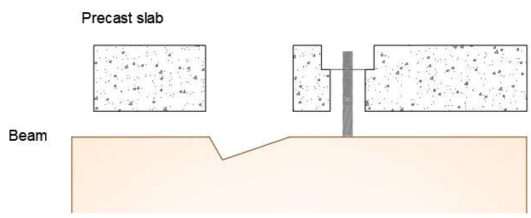

Figure 4: *Assembly timber elements and connectors with the precast concrete element*

After that, the steel plate, washer, and hex nut were added to the connector, to which a tightening was applied between the hex nut and the plate. It is important to note that immediately before the start of the test a tightening torque of 80Nm was applied, using a torque wrench.

The load procedure used for the static test was that indicated in standard EN26891 [13] (Figure 5).

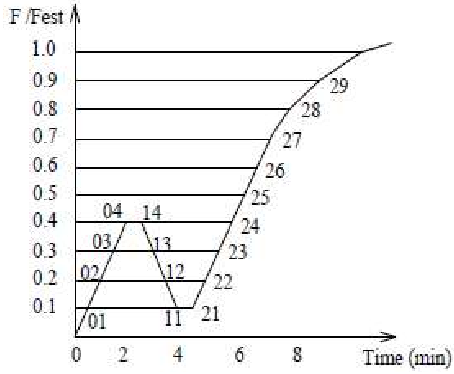

Figure 5: *Load procedure according to EN 26891[13]*

The cyclic tests were performed as follows: a load amplitude was applied between $0.1F_{est}$ and $0.3F_{est}$, with a frequency of 1Hz, i.e., one cycle per second. However, the test started with a pre-loading of $0.2F_{est}$ and was maintained for 10 seconds before the cyclic protocol started (50,000 cycles). The cycles were applied through a sinusoidal function. The loading procedure applied is shown in Figure 6.

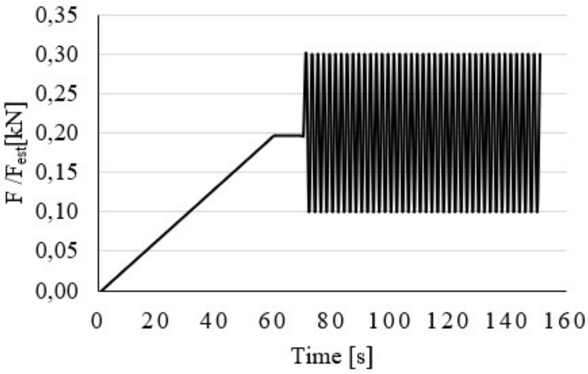

Figure 6: *Load procedure for cyclic test*

Before the cyclic and fatigue test, a static test was performed to calculate the initial stiffness of the connections, and at the end of the cyclic and fatigue test, the specimen was subjected to the static test where it was possible to determine the final stiffness and the failure load of the connection.

Figure 7 shows the load protocol used to determine the initial and intermediate stiffness in cyclic and fatigue tests.

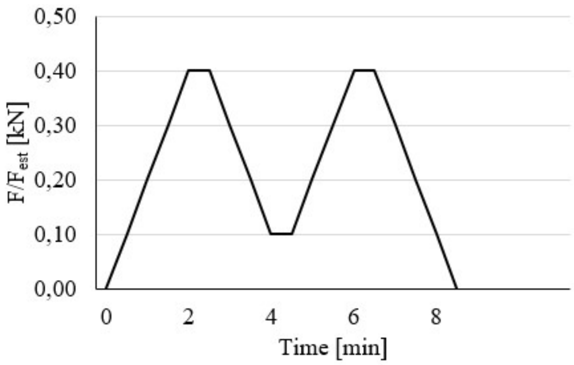

Figure 7: *Load procedure for initial and intermediate stiffness test*

Four cyclic tests were performed. The test protocol involved the following:

i) an initial static test to determine the initial stiffness;
ii) followed by the cyclic test with a total of 50,000 cycles;
iii) after which the specimen was loaded to failure following the static test protocol.

The fatigue tests were performed in a similar way to the cyclic tests; the only difference was the number of applied cycles: 1000,000 cycles. Along with the entire duration of the tests, a static test was performed, at each 24h period, to determine the intermediate stiffness. This procedure was used on fatigue tests due to the capacity of the system to save the data of tests.

Two fatigue tests were performed. The procedure was as follows:

i) started with a static test to determine the initial stiffness;
ii) followed by a cyclic test (about 85,000 cycles);
iii) after which an intermediate stiffness test was performed;
iv) the previous steps were repeated in sequence until reaching 1000,000 cycles;
v) after the number of cycles was completed, the static failure test was performed until failure.

During the tests, the load applied by the actuator and the relative displacement between the timber and concrete parts were recorded. The load capacity was recorded using a 500kN load cell. The relative displacement between timber and concrete were measured using 2 displacement transducers (LVDT 1 and LVDT 2) with a 50mm capacity, placed on both sides of the timber piece. Two LVDT's were also placed in the backside of timber pieces (LVDT 3 and LVDT 4) to measure the displacement or rotation that the specimen encountered during testing (Figure 8).

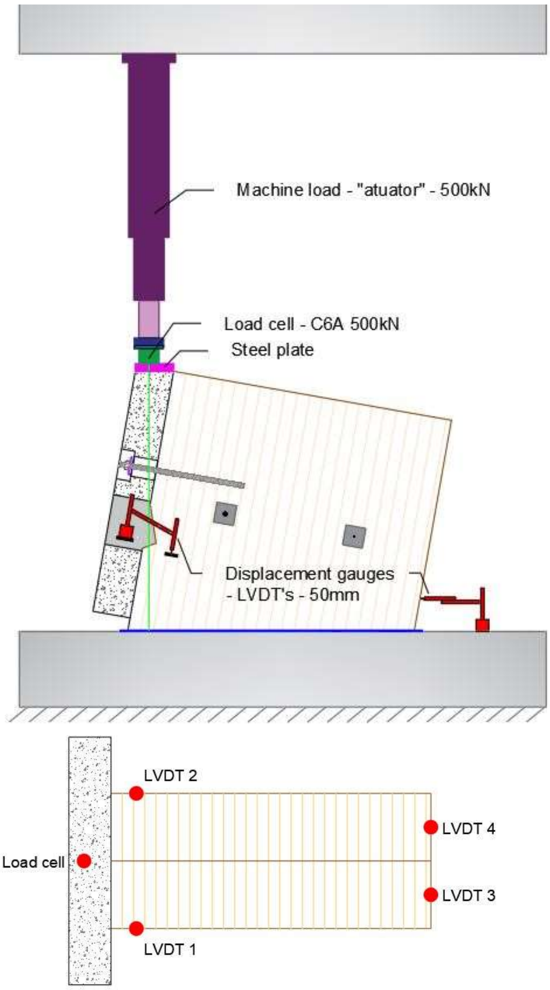

Figure 8: *Set-up of test and LVDT's position (in plan)*

3.1.2 RESULTS

The load capacity and the slip modulus were determined using the standard EN26891 [13]. Material characterization tests were also carried out (on timber beams and concrete).

For the timber elements the dynamic MOE, moisture content, and density were determined.

The dynamic MOE was determined through a longitudinal vibration test. The average dynamic MOE of the timber beam was 11699 N/mm^2, Figure 9 shows a timber beam in the test position.

Figure 9: *Timber beam of the composite in position to perform the dynamic assessment*

Density and moisture content tests were determined according to the procedures referred to in EN 13183-1 [14]. For the moisture content, an average value of 13.4% was obtained and for density, the average value obtained was 435.5 kg/m^3.

Concrete characterization tests were carried out, namely the compressive strength test, according to standard NP EN 206-1 [15]. The results are presented in Table 1.

Table 1: *Concrete characterization test results (concrete of class C30/37)*

f_{ck} [Mpa]		
At 14 days	At 31 days	At 196 days
31.0	37.1	41.1

Five preliminary static tests of the TCC elements were performed using symmetrical specimens composed of two timber beams with notches and with the concrete deck positioned in the centre. Figure 10 shows the load-displacement curves obtained in the preliminary tests; the average value obtained for stiffness (K_{ser}) was 1127 kN/mm/m. Specimen P.1 has a different load-displacement curve due to a secondary effect that could not be identified.

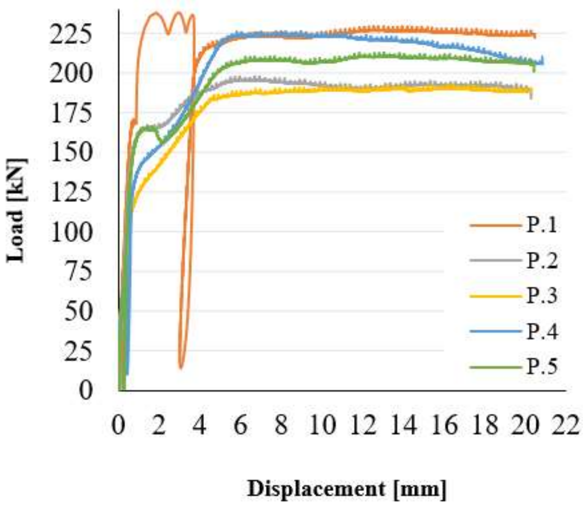

Figure 10: *Load-displacement curves obtained in the preliminary tests*

Six static tests, four cyclic tests, and two fatigue tests of the TCC elements were performed using asymmetrical specimens.

The results obtained (initial and final stiffness, and load capacity) in static, cyclic, and fatigue tests are shown in Table 2. The static tests are designated by "A.i"; the cyclic ones by "B.i" and fatigue ones by "C.i".

Table 2: Results of static, cyclic and fatigue tests

Push-out test specimen	$K_{ser,\ initial}$ [kN/mm]	$K_{ser,\ final}$ [kN/mm]	$F_{máx}$ [kN]
A1.1	1688.9	-	496.4
A1.2	628.5	-	481.8
A1.3	1052.8	-	499.3
A1.4	658.5	-	439.5
A1.5	505.4	-	413.4
A1.6	695.2	-	438.2
Average (A1.i)	871.5	-	461.4
Standard deviation	440.6	-	35.8
B1.1	881.1	2746.8	412.7
B1.2	619.8	1915.5	457.0
B1.3	399.8	1542.7	431.1
B1.4	173.1	508.5	386.7
Average (B1.i)	518.5	1678.4	421.9
Standard deviation	302.8	928.2	29.7
C1.1	455.0	1077.5	358.5
C1.2	240.5	496.2	322.1
Average (C1.i)	347.7	786.9	340.3
Standard deviation	151.7	411.0	25.7
All push-out test specimen			
Average	666.5	1831.2	428.1
Standard deviation	405.8	873.3	53.9

In all the tests performed, the combination of two possible types of failure was consistently observed: failure by shear in grout (*Sika Grout-218)* and failure by compression parallel to grain in the timber. Figure 11 shows the specimen and the failure obtained.

Figure 11: *Test specimen (before and after failure)*

- Static test:

From static tests performed on the six specimens, an average stiffness of 871.5 kN/mm and a failure load of 461.4kN were obtained. Figure 12 shows the load-displacement curves of the static tests. Specimen A1.1 and A1.3 have a higher stiffness compared to the other ones, and there are two possible reasons. For instance, one reasonable reason is that the applied torque may have been different because the torque wrench was not digital. Also, between the precast slab and the timber beams, it was not always possible to guarantee perfect contact between them, with a gap of millimetres between both elements.

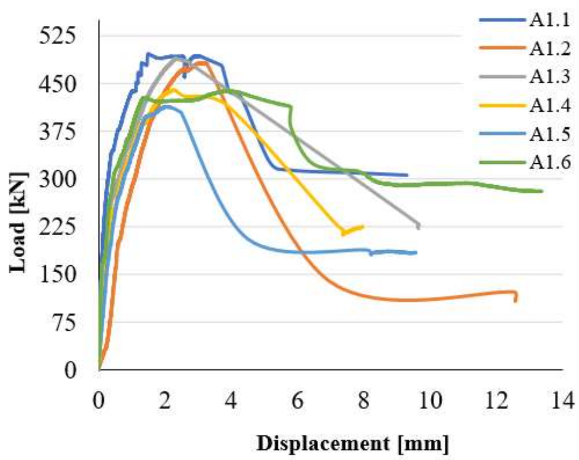

Figure 12: *Load-displacement curves (of the static test)*

- Cyclic test:

From cyclic tests performed on the four specimens an initial average stiffness obtained was 518.5kN/mm and a final average stiffness was 1678.4kN/mm, corresponding to an increase of 223.7%. The failure load obtained after the 50,000 cycles was 421.9kN which is 8.6% lower than the average failure load obtained in static tests (A1.i) without cycles. In general, the stiffness increases with the application of the cycles, but the ultimate load decreases and presents a much brittle failure with respect to the static test (series A1.i) as shown in Figure 13 and Figure 14, Figure 12 corresponding to the load-displacement curves of the initial stiffness test and the final-static test.

The increase in stiffness with the number of cycles is a predictable behaviour, and the results of the cycle tests confirmed this. In comparison to static tests (series A1.i), the average initial stiffness has increased by 92.6%, and the average final stiffness has increased by 223.7%.

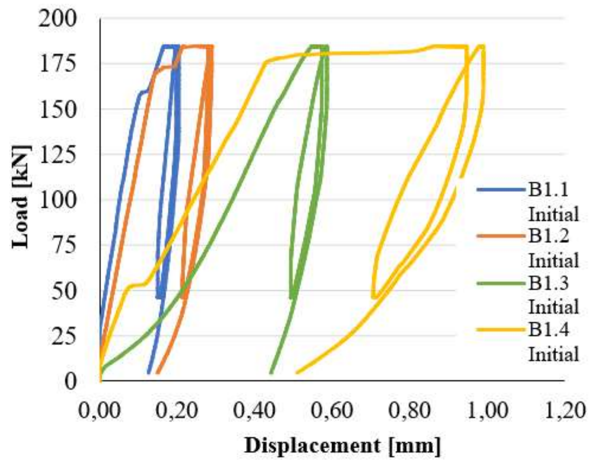

Figure 13: *Load – displacement curves (of the cyclic tests) corresponding to the initial stiffness test protocol)*

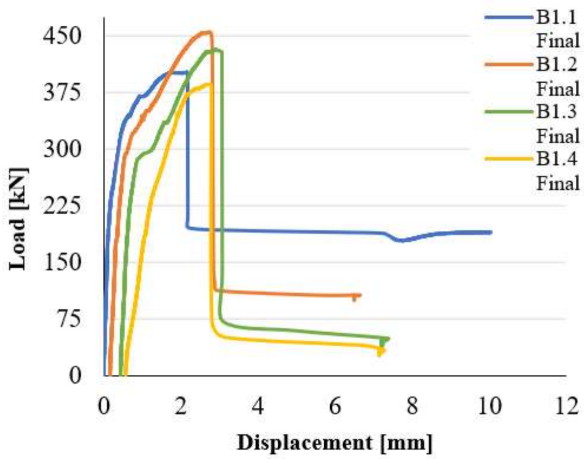

Figure 14: *Load-displacement curves (of the cyclic tests) corresponding to the final static test protocol up to failure*

Figure 15 shows ruptures obtained in the final static test after the cyclic test. It is possible to see the rupture that occurred in the timber beams and the concrete slab. The type of rupture was similar to the ones observed in the static tests. Additionally, cracking of the concrete slab in the bonding area was observed in these tests.

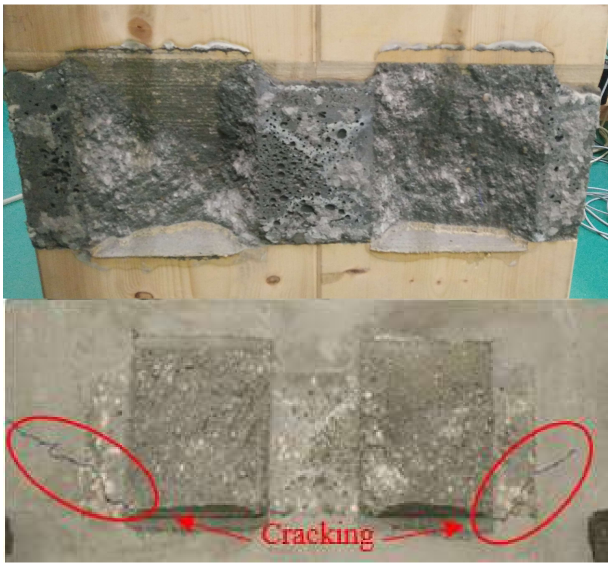

Figure 15: *Ruptures obtained (timber and concrete side)*

- Fatigue test:

From fatigue tests performed on the two specimens an initial average stiffness obtained was 347.7kN/mm and a final average stiffness was 786.9kN/mm, corresponding to an increase of 126.3%. The failure load obtained after the 1000,000 cycles was 340.3kN which is 26.3% lower than the average failure load obtained in static tests (A1.i) without cycles and which is 19.3% lower than the average failure load obtained in final static tests after 50,000 cycles (series B1.i). As with the cyclic tests, the failure load decreases as the number of cycles increases.

Concerning average stiffness, the difference between fatigue (series C1.i) and static tests (series A1.i) was 9.7%, and the difference between cyclic (series B1.i) and fatigue tests (series C1.i) was 53.1%.

Figure 16 shows the load-displacement curves of the initial stiffness test protocol and final static test protocol up to the failure of the fatigue tests.

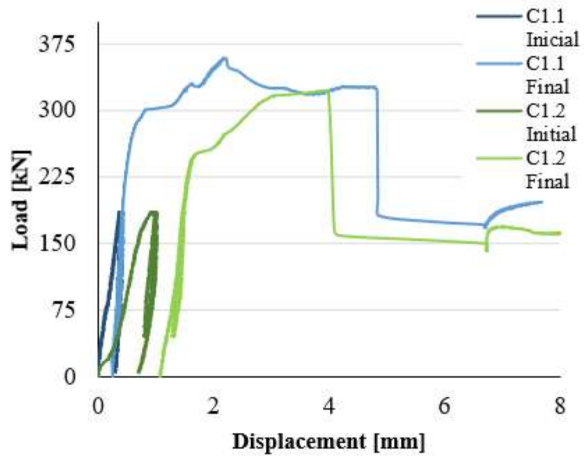

Figure 16: *Load - displacement curves (of the fatigue tests) corresponding to the initial stiffness test protocol and final static test protocol up to failure*

Figure 17 shows the curves of evolutions of stiffness obtained during the fatigue tests.

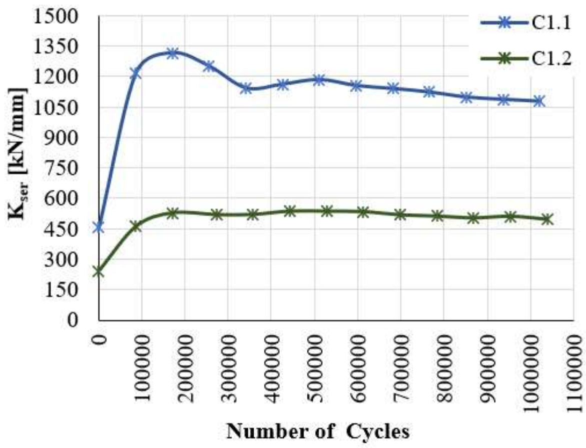

Figure 17: *Evolution of stiffness obtained during the fatigue test*

The results given in the previous figures clearly indicate a similar performance in both tested specimens, specimen C1.1 presenting the higher stiffer. As with the cyclic tests, the stiffness increases with the increases in the number of cycles, at least up, approximately, 200,000 cycles. Between these and 500,000 cycles there was a decrease in stiffness. After the 500,000 cycles, there was an almost constant stiffness. The difference between first stiffness and the stiffness obtained after approximately 84,000 cycles is 140.1% and 55% between initial and final stiffness.

During the fatigue test of specimen C1.2, at 850,000 cycles, a noise was heard near one of the notches, where it is believed that the failure occurred due to shear in the grout. That is why the value of the stiffness in this specimen is lower. It is not possible to say whether this rupture would have occurred before. However, this did not significantly affect the failure load value.

Figure 18 shows the evolution of the average value of the failure load in the test, with the increase in the number of cycles considered (i.e., 1 cycle – series A, 50,000 cycles – series B, and 1000,000 cycles – series C). The failure load decreases as the number of cycles increases as expected.

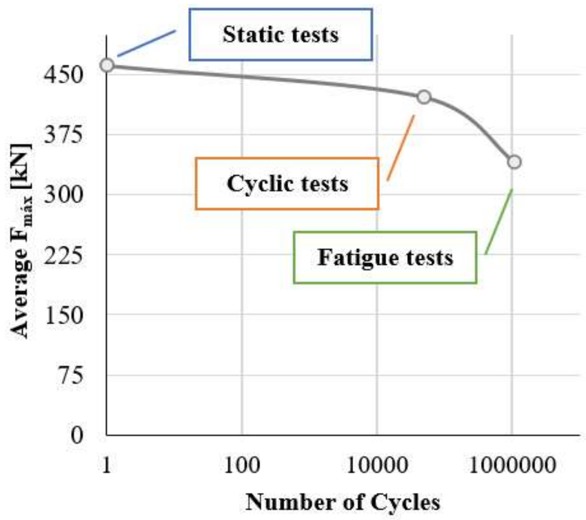

Figure 18: *Average value of the failure load obtained in the different type of tests (static, cyclic, and fatigue)*

4 CONCLUSIONS

The set of tests performed revealed that the failure mode was the same in all specimens, independent of the type of test performed (solo static, cyclic, or fatigue) and thus the application of cyclic loads or the number of cycles in the connection does not influence the type of collapse of the connection system. However, in the cyclic and fatigue tests, cracking on the concrete surface was additionally observed.

From the analysis of the set of tests, it was concluded that the load capacity of the connection is not significantly affected. There was an 8.6% reduction in the average load carrying capacity obtained in the cyclic tests with respect to the static ones; between static and fatigue tests a 26.3% reduction, and a 19.3% reduction between cyclic and fatigue tests.

From the analysis of the set of tests, it was concluded that the stiffness of the connection is affected. the average stiffness of cyclic tests increases by 92.6% as compared to the static ones; the fatigue tests were reduced by 9.7%, and cyclic and fatigue tests were reduced by 53.1%.

Regarding the connection stiffness, it is concluded that there is an increase in stiffness with the number of cycles, up to a certain level of load cycles, after which it reduces. After applying 50,000 cycles there was an average increase of 223.7% in stiffness with respect to the initial static stiffness.

In the case of fatigue tests, there was also a 140.1% increase in stiffness between the first stiffness and the stiffness obtained after approximately 84,000 cycles, when comparing the initial stiffness with the final stiffness there is an increase of about 55%.

Additional test results are pending in a comprehensive final report to be available soon.

REFERENCES

[1] Wacker J.P., Dias A.M.P.G., Hosteng T. 100 Years Performance of Timber-Concrete-Composite Bridges in the USA. J Bridge Eng., 25 (3):04020006, 2020;
[2] Rodrigues J.N., Dias A.M.P.G., Providencia P. Timber-Concrete Composite Bridges: State-of-the-Art Review. Bioresources. 2013;8:6630-49.
[3] Rodrigues J.N., Providencia P., Dias A.M.P.G. Sustainability and Lifecycle Assessment of Timber-Concrete Composite Bridges. Journal of Infrastructure Systems. 2017;23.
[4] Cen. Eurocode 1 - General actions - Part 1-1: Densities, self-weight, imposed loads for buildings Brussels: CEN; 2002.
[5] Cen. Eurocode 0 - Basis of structural design. Brussels: CEN; 2002.
[6] C. Eurocode 5 - Design of timber structures - Part 1-2: General - Structural fire design. Brussels: CEN; 2004.
[7] Cen. Eurocode 5 - Design of timber structures - Part 2: Bridges. Brussels: CEN; 2004.
[8] Cen. Eurocode 5 - Design of timber structures - Part 1-1: General - Common rules and rules for buildings. Brussels: CEN; 2004.
[9] Cen. Eurocode 2 - Design of concrete structures - Part1-1: General rules and rules for buildings. Brussels: CEN; 2010.
[10] AASHTO. AASHTO-LRFD bridge design specifications. 8th edition. 2019. Washington, DC: American Association of State, Highway, and Transportation Officials.
[11] Monteiro S.R.S., Dias A.M.P.G., Negrao J.H.J.O. Assessment of Timber-Concrete Connections Made with Glued Notches: Test Set-Up and Numerical Modeling. Experimental Techniques. 2013;37:50-65.
[12] Dias A.M.P.G. Analysis of the Nonlinear Behavior of Timber-Concrete Connections. J Struct Eng. [2]2012;138:1128-37.
[13] CEN, EN 26891 - Timber structures - Joints made with mechanical fasteners - general principles for the determination of strength and deformation characteristic. Brussels: CEN, 1991.
[14] CEN, EN 13183-1 - Moisture content of a piece of sawn timber - Part 1: Determination by oven dry method. Brussels: CEN, 2002.
[15] CEN, NP EN 206:2013+A1:2017 - Betão; Especificações, desempenho, produção e conformidade. Brussels: CEN, 2017

In: Proceedings of the World Conference on Timber Engineering, August 9-12, 2021, Santiago, Chile. Paper No: TE0414-1.